Vertical Jump Height Estimation Algorithm based on Vertical Acceleration Profile Characteristics via Foot-Worn Inertial Sensing

Article *in* Journal of Biomechanical Engineering · December 2017

DOI: 10.1115/1.4038740

CITATIONS
0

READS
203

3 authors:

Jianren Wang
Carnegie Mellon University
10 PUBLICATIONS **33** CITATIONS
SEE PROFILE

Junkai Xu
Shanghai Jiao Tong University
11 PUBLICATIONS **72** CITATIONS
SEE PROFILE

Peter B Shull
Shanghai Jiao Tong University
73 PUBLICATIONS **1,041** CITATIONS
SEE PROFILE

Vertical Jump Height Estimation Algorithm Based on Takeoff and Landing Identification Via Foot-Worn Inertial Sensing

Jianren Wang
State Key Laboratory of Mechanical System and Vibration,
School of Mechanical Engineering,
Shanghai Jiao Tong University,
800 Dongchuan Road,
Shanghai 200240, China
e-mail: wangxingyuan@sjtu.edu.cn

Junkai Xu
State Key Laboratory of Mechanical System and Vibration,
School of Mechanical Engineering,
Shanghai Jiao Tong University,
800 Dongchuan Road,
Shanghai 200240, China
e-mail: abcyxjk@sjtu.edu.cn

Peter B. Shull[1]
State Key Laboratory of Mechanical System and Vibration,
School of Mechanical Engineering,
Shanghai Jiao Tong University,
800 Dongchuan Road,
Shanghai 200240, China
e-mail: pshull@sjtu.edu.cn

Vertical jump height is widely used for assessing motor development, functional ability, and motor capacity. Traditional methods for estimating vertical jump height rely on force plates or optical marker-based motion capture systems limiting assessment to people with access to specialized laboratories. Current wearable designs need to be attached to the skin or strapped to an appendage which can potentially be uncomfortable and inconvenient to use. This paper presents a novel algorithm for estimating vertical jump height based on foot-worn inertial sensors. Twenty healthy subjects performed countermovement jumping trials and maximum jump height was determined via inertial sensors located above the toe and under the heel and was compared with the gold standard maximum jump height estimation via optical marker-based motion capture. Average vertical jump height estimation errors from inertial sensing at the toe and heel were -2.2 ± 2.1 cm and -0.4 ± 3.8 cm, respectively. Vertical jump height estimation with the presented algorithm via inertial sensing showed excellent reliability at the toe ($ICC_{(2,1)} = 0.98$) and heel ($ICC_{(2,1)} = 0.97$). There was no significant bias in the inertial sensing at the toe, but proportional bias ($b = 1.22$) and fixed bias ($a = -10.23$cm) were detected in inertial sensing at the heel. These results indicate that the presented algorithm could be applied to foot-worn inertial sensors to estimate maximum jump height enabling assessment outside of traditional laboratory settings, and to avoid bias errors, the toe may be a more suitable location for inertial sensor placement than the heel. [DOI: 10.1115/1.4038740]

1 Introduction

Vertical jump height is often used to assess motor development, functional ability, and motor capacity, in the young [1,2], elderly [3–5], and athletes [6–9]. Vertical jump height has been linked to anaerobic power and capacity in medical applications [10] and sports training [8,11] and is frequently assessed in sports where jumping is a critical skill such as in basketball for shooting, blocking, and rebounding [9]. Some health care professionals have used training techniques to improve vertical jump performance to prevent lower extremity injuries [12], and vertical jump has also been used as a functional test to determine the success of different treatment methods postoperatively [13].

Two primary methods have been employed to estimate jump height: (1) direct measurement of vertical displacement and (2) indirect measurement through flight phase estimation. In the first method, vertical displacement is directly measured at a body landmark, such as the hand [14,15], waist [16], head [17], or center of mass [18–20], and the vertical displacement trajectory is computed as the position of the body landmark over time during the flight phase of jumping with respect to the stationary standing position [14–20]. This direct method is simple and accurate and is considered the gold standard for assessing vertical jump height [20,21]; however, it is limited to the relatively few people who have access to motion capture facilities. In the second method, vertical jump height is indirectly estimated, without the need to track position trajectories, by applying the equation of free-falling motion during flight, and takeoff velocity and/or flight time are used to estimate the jump height [22–25]. The flight time equation, $h = (1/8) \times (\text{flight time})^2 \times g$, has been used in isolation [22,23], the takeoff velocity equation, $h = (1/2) \times (\text{take off velocity})^2/g$, has been used in isolation [24], and both flight time and takeoff velocity have been used in combination, $h = (\text{take off velocity}) \times (\text{flight time}) - (1/2) \times (\text{flight time})^2 \times g$ [25], to estimate vertical jump height.

Laboratory-based sensing devices have long been used to estimate jump height. Bosco et al. [23] used basic particle kinematics equations to calculate jump height from flight time by optical cells and contact mats. Similarly, Just Jump System [15] estimated the time interval from takeoff to landing via microswitches embedded in a mat. Bobbert and Van Soest [21] used motion capture with passive markers to calculate the position and velocity of the mass center of the body and computed jump height as the height difference between the apex of the jump and a standing upright position. Similarly, Pandy and Zajac [20] used motion capture with active markers to track absolute displacement of the body center of mass to compute jump height. Besides, there are existing simple equipment options for estimating vertical jump height; however, these devices are typically large, bulky, and not easily moved [15,26].

One compelling benefit of using a wearable sensing approach is that jump height could potentially be performed in the field or on the court during practice and games, and thus, provides key insights into injury diagnosis/prevention [27] and improving performance [28]. Tri-axial accelerometers placed on the ankle, sacrum, trunk, thigh, and shank have been used to compute jump height by applying the equation of free-falling motion and estimating flight time from accelerometer signals [27,29–31]. Another approach is to double integrate the acceleration magnitude on the sacrum to estimate a vertical trajectory profile [32].

One drawback of current wearable designs is that they need to be attached to the skin or strapped to an appendage which can potentially be uncomfortable and inconvenient to use. In contrast, a foot mounted-accelerometer approach is portable and could be used in a variety of settings such as gymnasiums [33], the field [34–36], laboratories [37], research clinics [38,39], or even at home [40]. However, there are currently no validated foot-worn sensor algorithms for estimating vertical jump height. Therefore, the purpose of this paper is to present a vertical jump height estimation algorithm based on foot-worn inertial sensing. Recent

[1]Corresponding author.
Manuscript received December 10, 2016; final manuscript received November 19, 2017; published online January 23, 2018. Assoc. Editor: Paul Rullkoetter.

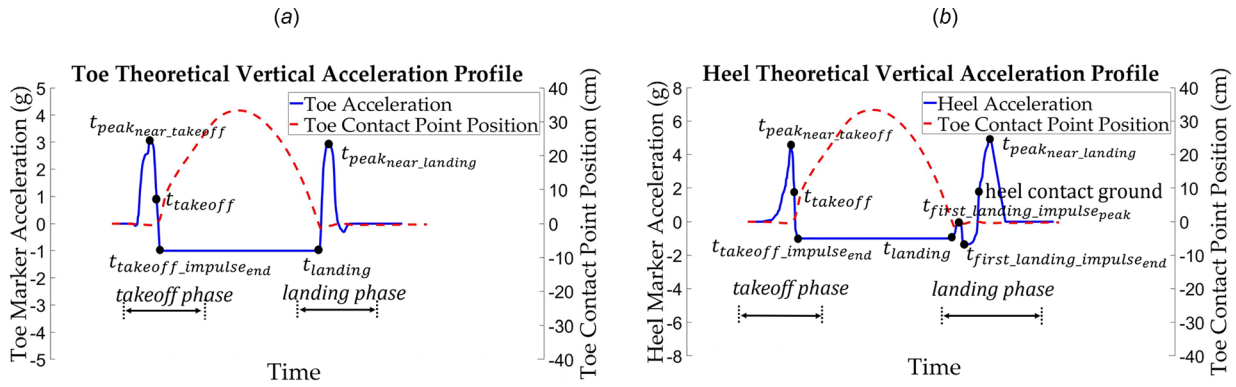

Fig. 1 (*a*) Toe theoretical vertical acceleration profile and (*b*) heel theoretical vertical acceleration profile for a vertical jump for a 75 kg healthy male subject based on the OpenSim Sky Higher: Dynamic Optimization of Maximum Jump Height [42]. Vertical upward position and acceleration are positive.

work has shown that there is a linear relationship between estimating vertical jump height with a force platform based on the flight time equation and estimating vertical jump height with motion capture (considered the gold standard) based on center of mass displacement [41]. Following a similar principle, we hypothesize this linear relationship between the flight-time equation and center of mass displacement can be applied to foot-worn inertial sensing and build an algorithm around this idea. We first introduce the vertical jump height estimation algorithm based on foot-worn inertial sensing at the toe and heel and then present validation testing and results and discuss implications of these findings.

2 Vertical Jump Height Estimation Algorithm

The countermovement jump, a most common jump movement in many sports such as volleyball and basketball and often used as a benchmark metric [9], is characterized by an individual starting from an upright standing position, making a preliminary downward movement by flexing the knees and hips, and then immediately extending the knees and hips again to leap vertically from the ground. The countermovement jump makes use of the stretch-shorten cycle, where the muscles are prestretched before shortening in the desired direction [10]. Maximum vertical jump height of the countermovement jump is the focus of this algorithm.

The presented algorithm is based on the estimated vertical acceleration in the world frame at the toe and heel. To understand the relationship between acceleration and position, we determine theoretical toe and heel acceleration profiles during a vertical jump, through OpenSim 3.3 dynamic simulation [42]. The standard musculoskeletal model Gait2392_simbody was used and the "Sky Higher: Dynamic Optimization of Maximum Jump Height" [42] simulation was modified to compute toe and heel vertical position and acceleration profiles during vertical jump simulations. In the model, the subject was a 75 kg healthy male, the toe marker was located at the extremity of the second proximal phalanx, the heel marker was located at the calcaneus and the toe contact point was located at the tip of the second distal phalanx.

2.1 Theoretical Vertical Acceleration Profile. The toe theoretical vertical acceleration profile (Fig. 1(*a*)), determined from the simulation described earlier, displays the three distinct phases of vertical jumps: takeoff, flight, and landing [27,29,30]. The feet initially plantar flex producing an acceleration impulse that reaches a peak ($t_{\text{peak}_{\text{near\_takeoff}}}$) just prior to takeoff (t_{takeoff}). During flight, the impulse quickly ends ($t_{\text{takeoff}_{\text{impulse\_end}}}$) and assuming no ankle rotation after the impulse, the toe theoretically experiences -1 g acceleration. Following the flight phase, the toe experiences another acceleration impulse starting at the point of initial toe contact with the ground (t_{landing}). This impulse during the landing phase quickly reduces the speed of downward vertical movement and reaches another peak($t_{\text{peak}_{\text{near\_landing}}}$).

Similarly, the heel theoretical vertical acceleration profile (Fig. 1(*b*)) also displays the three distinct phases of vertical jumps: takeoff, flight, and landing. The feet initially plantar flex producing an acceleration impulse that reaches a peak ($t_{\text{peak}_{\text{near\_takeoff}}}$)just prior to takeoff ($t_{\text{takeoff}}$). During flight, the impulse quickly ends ($t_{\text{takeoff}_{\text{impulse\_end}}}$) and assuming no ankle rotation, the heel theoretically experiences -1 g acceleration. Following the flight phase, the heel experiences another two acceleration impulses: (1) the first one starts at the point of initial toe contact with the ground (t_{landing}), and (2) the second one is produced by heel downward rotation that reaches a peak ($t_{\text{peak}_{\text{near\_landing}}}$) just after heel contact with the ground. The second impulse during the landing phase quickly reduces the speed of heel downward movement.

In this work, takeoff was defined as the instant when the toe contact point lost contact with the ground, landing was defined as the instant when the toe contact point contacted the ground again, and flight was defined as the time between takeoff and landing [27,29,30].

2.2 Vertical Jump Height Algorithm Based on Acceleration. The vertical jump height algorithm is composed of six components (Fig. 2). Peak detection is performed to find maximum acceleration timepoints and landing phases [29]. Distinct acceleration characteristics within the takeoff and landing phases are used to estimate specific takeoff and landing times. Finally, vertical jump height is estimated via flight-time equations [23].

2.2.1 Peak Detection. According to the vertical jump simulation results described earlier, the takeoff and landing phases can be characterized by the presence of vertical acceleration $a(t)$peaks ($t_{\text{peak}_{\text{near\_takeoff}}}$ and $t_{\text{peak}_{\text{near\_landing}}}$ in Figs. 1(*a*) and 1(*b*)). Thus, the instant of the absolute maximum value (t_1) can be defined either in the takeoff or landing phase

$$t_1 = \text{argmax}(a(t)), (\text{trial\_start\_time} < t < \text{trial\_end\_time}) \quad (1)$$

Then, to detect the phase that t_1 belongs to, it is necessary to assess the instant t_2 of the absolute maximum value, outside the interval $[t_1 - T_m/2, t_1 + T_m/2]$, where T_m is the maximum range of takeoff and landing phases

$$t_2 = \arg\max(a(t)), \left(t < t_1 - \frac{T_m}{2}, t > t_1 + \frac{T_m}{2}\right) \quad (2)$$

T_m was set to 200 ms based on previous findings [29]. If t_1 occurs first, it belongs to the takeoff phase, and t_2 belongs to the landing phase. If t_2 occurs first, the reverse is true. Thus, the time of the maximum peak during takeoff and landing is

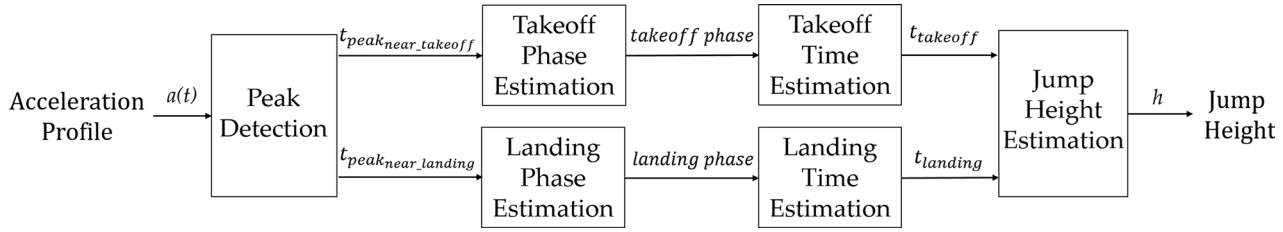

Fig. 2 Vertical jump height estimation algorithm. Peak detection is performed to find maximum acceleration values and, in turn, to determine takeoff and landing phases. Distinct acceleration characteristics within the takeoff and landing phases are used to estimate specific takeoff and landing times. Finally, vertical jump height is estimated via flight-time equations.

$$t_{\text{peak}_{\text{near\_takeoff}}} = \min(t_1, t_2) \tag{3}$$

$$t_{\text{peak}_{\text{near\_landing}}} = \max(t_1, t_2) \tag{4}$$

2.2.2 Takeoff and Landing Phase Estimation. To ensure takeoff and landing instants are properly identified and to eliminate the effects of resonance, takeoff and landing phases should be determined based on takeoff and landing impulses. To determine takeoff and landing phases, the maximum durations of each were set based on previous research to $T_{\text{max\_takeoff\_interval}} = 160\,\text{ms}$ and $T_{\text{max\_landing\_interval}} = 200\,\text{ms}$ [29]. Thus, the takeoff and landing phases are defined as

$$\text{takeoff phase} = \left[t_{\text{peak}_{\text{near\_takeoff}}} - \frac{T_{\text{max\_takeoff\_interval}}}{2}, t_{\text{peak}_{\text{near\_takeoff}}} + \frac{T_{\text{max\_takeoff\_interval}}}{2}\right] \tag{5}$$

$$\text{landing phase} = \left[t_{\text{peak}_{\text{near\_landing}}} - \frac{T_{\text{max\_landing\_interval}}}{2}, t_{\text{peak}_{\text{near\_landing}}} + \frac{T_{\text{max\_landing\_interval}}}{2}\right] \tag{6}$$

2.2.3 Takeoff Time Estimation. According to the vertical jump simulation results described earlier, takeoff occurs after the acceleration impulse in the takeoff phase and is approximately coincident with the midpoint of the falling edge of the acceleration impulse in the takeoff phase, whose beginning time is $t_{\text{peak}_{\text{near\_takeoff}}}$. Thus, it is necessary to detect the end time of the acceleration impulse during the takeoff phase, $t_{\text{takeoff}_{\text{impulse\_end}}}$, and $t_{\text{takeoff}_{\text{impulse\_end}}}$ is approximately coincident with the minimum acceleration in the interval $[t_{\text{peak}_{\text{near\_takeoff}}}, t_{\text{peak}_{\text{near\_takeoff}}} + T_{\text{max\_takeoff\_interval}}/2]$

$$t_{\text{takeoff}_{\text{impulse\_end}}} = \arg\min(a(t)) \times \left(t_{\text{peak}_{\text{near\_takeoff}}} < t < t_{\text{peak}_{\text{near\_takeoff}}} + \frac{T_{\text{max\_takeoff\_interval}}}{2}\right) \tag{7}$$

Then, the takeoff instant t_{takeoff} can be determined as the arithmetic mean of $t_{\text{peak}_{\text{near\_takeoff}}}$ and $t_{\text{takeoff}_{\text{impulse\_end}}}$

$$t_{\text{takeoff}} = \frac{1}{2} \times \left(t_{\text{peak}_{\text{near\_takeoff}}} + t_{\text{takeoff}_{\text{impulse\_end}}}\right) \tag{8}$$

Takeoff time estimation was the same for both toe and heel acceleration as their profiles share the same general pattern (Figs. 1(*a*) and 1(*b*)).

2.2.4 Landing Time Estimation. According to the vertical jump simulation results described earlier, the toe experiences an acceleration impulse starting at the point of initial contact during landing. Thus, it is necessary to detect the beginning time t_{landing} of the acceleration impulse in the landing phase. According to the toe theoretical vertical acceleration profile, t_{landing} is approximately coincident with the minimum in the interval $[t_{\text{peak}_{\text{near\_landing}}} - T_{\text{max\_landing\_interval}}/2, t_{\text{peak}_{\text{near\_landing}}}]$

$$t_{\text{landing}} = \arg\min(a(t)) \left(t_{\text{peak}_{\text{near\_landing}}} - \frac{T_{\text{max\_landing\_interval}}}{2} < t < t_{\text{peak}_{\text{near\_landing}}}\right) \tag{9}$$

Takeoff time estimation based on heel acceleration is more complicated, since the heel experiences two acceleration impulses during the landing phase (Fig. 1(*b*)). Landing is coincident with the instant t_{landing} of the beginning time of the first acceleration impulse in landing phase, which can be detected via the following steps: (1) detect the end $t_{\text{first\_landing\_impulse}_{\text{end}}}$ of the first acceleration impulse in the landing phase, (2) detect the time $t_{\text{first\_landing\_impulse}_{\text{peak}}}$ when the first landing impulse reaches a peak, and (3) detect the beginning time of the first acceleration impulse in landing phase t_{landing}.

According to the heel theoretical vertical acceleration profile, the end time of the first acceleration impulse in the landing phase can be found at the instant of minimum acceleration in the interval $[t_{\text{peak}_{\text{near\_landing}}} - T_{\text{max\_landing\_interval}}/2, t_{\text{peak}_{\text{near\_landing}}}]$

$$t_{\text{first\_landing\_impulse}_{\text{end}}} = \arg\min(a(t)) \times \left(t_{\text{peak}_{\text{near\_landing}}} - \frac{T_{\text{max\_landing\_interval}}}{2} < t < t_{\text{peak}_{\text{near\_landing}}}\right) \tag{10}$$

Then, the peak of the first acceleration impulse in the landing phase can be found at the instant of maximum acceleration in the interval $[t_{\text{peak}_{\text{near\_landing}}} - T_{\text{max\_landing\_interval}}/2, t_{\text{first\_landing\_impulse}_{\text{end}}}]$

$$t_{\text{first\_landing\_impulse}_{\text{peak}}} = \arg\max(a(t)) \times \left(t_{\text{peak}_{\text{near\_landing}}} - \frac{T_{\text{max\_landing\_interval}}}{2} < t_{\text{first\_landing\_impulse}_{\text{end}}}\right) \tag{11}$$

Finally, the beginning time of the first acceleration impulse in landing phase can be found at the instant t_{landing} of minimum acceleration in the interval $[t_{\text{peak}_{\text{near\_landing}}} - T_{\text{max\_landing\_interval}}/2, t_{\text{first\_landing\_impulse}_{\text{peak}}}]$

$$t_{\text{landing}} = \arg\min(a(t)) \times \left(t_{\text{peak}_{\text{near\_landing}}} - \frac{T_{\text{max\_landing\_interval}}}{2} < t < t_{\text{first\_landing\_impulse}_{\text{peak}}}\right) \tag{12}$$

2.2.5 Jump Height Estimation. Flight time T_f can be calculated based on takeoff time t_{takeoff} and landing time t_{landing} as

$$T_f = t_{\text{landing}} - t_{\text{takeoff}} \tag{13}$$

Once flight time is known, vertical jump height can be estimated via flight-time equations. The height of a vertical jump is directly related to the time the body is in the air and can be deduced from flight time T_f, via the ballistic formula [23]

$$H_{\text{Flight time}} = \frac{1}{2} \times \left(\frac{T_f}{2}\right)^2 \times g = \frac{1}{8} \times T_f^2 \times g \tag{14}$$

where g is the acceleration of gravity. It has been shown that there is a linear relationship between $H_{\text{Flight time}}$ and $H_{\text{Direct measurement}}$, which can be described by the following equation:

$$H_{\text{Direct measurement}} = \Delta_h + k_h \times H_{\text{Flight time}} \tag{15}$$

where k_h is approximated as 1 [41]. Δ_h is the vertical displacement between normal standing posture and the posture at toe-off, which is primarily due to ankle plantar flexion, and based on previous research this value can be set to 12 cm [27,41].

Therefore, vertical jump height, h, can be determined via the following equation:

$$h = \Delta_h + k_h \times \left(\frac{1}{8} \times T_f^2 \times g\right) \tag{16}$$

2.3 Assumption and Approximation in Algorithm. To develop and validate the general framework of the algorithm, we determined theoretical toe and heel acceleration profiles during a vertical jump, through OpenSim dynamic simulation. Takeoff and landing phase estimation were included to compensate for resonances that were not present in the theoretical acceleration profiles from OpenSim. After applying phase detection, the effects of resonance can be mitigated since the amplitude of resonance does not generally exceed the peak or trough during the takeoff/landing impulse in takeoff/landing phase. Thus, the resonance did not affect the detection of takeoff/landing characteristics as well as the accuracy of the algorithm.

The takeoff instant was chosen based on simulated, theoretical acceleration profiles. Takeoff was defined as the instant when the toe contact point lost contact with the ground. In the simulation, the takeoff instant is coincident with 56% of the falling edge. However, this result is based on simulation and may be slightly different when apply to different subjects. To simplify to calculation, we set it to the midpoint of falling edge.

3 Validation Testing

3.1 Subjects. To quantify the accuracy of the algorithm, 20 healthy subjects (14 males/six females, age: 24.5 ± 5.5 yr, height: 172.9±16.7 cm) participated in this study after giving informed consent in accordance with the Declaration of Helsinki. Potential subjects were excluded if they had undergone surgery after Achilles tendon rupture or had previous injuries to the ankle, knee, or hip.

3.2 Foot-Worn Inertial Sensing. Two electronic modules were used with a standard running shoe (2015SS, Skechers) to capture foot acceleration profiles during vertical jumping (Fig. 3). One module was taped to the top of the shoe above the head of the second metatarsal, and one module was inserted in the sole of the shoe under the heel. Each electronic module consisted of a microcontroller (ATmega32U4, Atmel Microcontrollers), nine-axis inertial measurement unit (BNO055, Bosch Sensortec), 500 mAh lithium-ion battery, and microSD card (microSDHC Class4, SanDisk). Inertial sensor data were sampled and stored at 200 Hz, which is sufficient to estimate peak vertical jump height [25]. Each module was encased in plastic and the overall size and weight were 55 × 48 × 15 mm and 52 g, respectively. For this

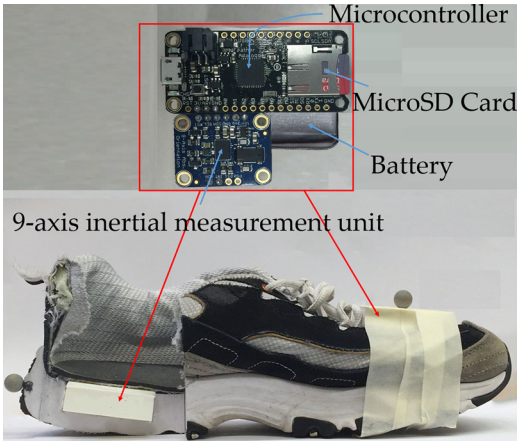

Fig. 3 Two electronic modules were used with a standard running shoe to capture foot acceleration profiles during vertical jumping. One module was taped to the top of the shoe above the head of the second metatarsal, and one module was inserted in the sole of the shoe under the heel. Each electronic module consisted of a microcontroller, nine-axis inertial measurement unit, 500 mAh lithium-ion battery, and microSD card.

study, only the vertical component of acceleration in the global frame at each time-step (determined through the proprietary Bosch Sensortec FusionLib library) was used for estimating vertical jump height. The Bosch Sensortec FusionLib has been validated with the sensors used in this paper and other Bosch sensors [43–45].

3.3 Experimental Testing. An optoelectronic motion capture system (Vicon, Oxford, UK) was used to collect raw position data at 200 Hz, which is a high enough sampling rate to accurately capture the peak jump height [27]. Four markers were placed around the waist: two were placed on the anterior superior iliac spines and two on the anterior inferior iliac spines. Subjects initially performed three practice jumps prior to data collection. Subjects then performed three vertical jump trials. For each trial, subjects started by standing on flat ground and then vertically jumped as high as they could. Between each trial, subjects were given a 1-min rest interval or longer if desired. During these jumps, measurements of body kinematics were collected simultaneously by the wearable shoe sensors and the motion capture system.

3.4 Data Analysis. The gold standard vertical jump height was computed via the motion capture system by averaging the heights of anterior superior iliac spine and anterior inferior iliac spine markers to determine absolute displacement of the body center of mass between the apex of the jump and the standing upright position [20]. Vertical jump height estimations from the inertial sensors were applied via the vertical jump height estimation algorithm described earlier. The mean and standard deviation of inertial sensor estimation errors were calculated. A two-way, random-effects, single measure intraclass correlation coefficients (ICC(2,1)) model was used to assess reliability of inertial sensor-based jump height estimates and point estimates of the ICCs were interpreted as follows: excellent (0.75–1), modest (0.4–0.74), or poor (0–0.39) [46]. Linear regression analysis [47] was performed to detect the proportional bias and fixed bias between the motion capture system and the inertial sensor at the toe and heel. The regression model is $E(A) = a + b(B$, where E is a symbol of function related to the difference between vertical jump height estimated using the presented algorithm and gold standard method. A is the vertical jump height estimation via foot-worn inertial sensing, B is the gold standard estimation via optical marker-based motion capture system. Proportional bias was determined as follows: 95% confidence interval (CI) for slope (b) does not include 1. And, fixed bias was determined as follows: 95% CI for intercept

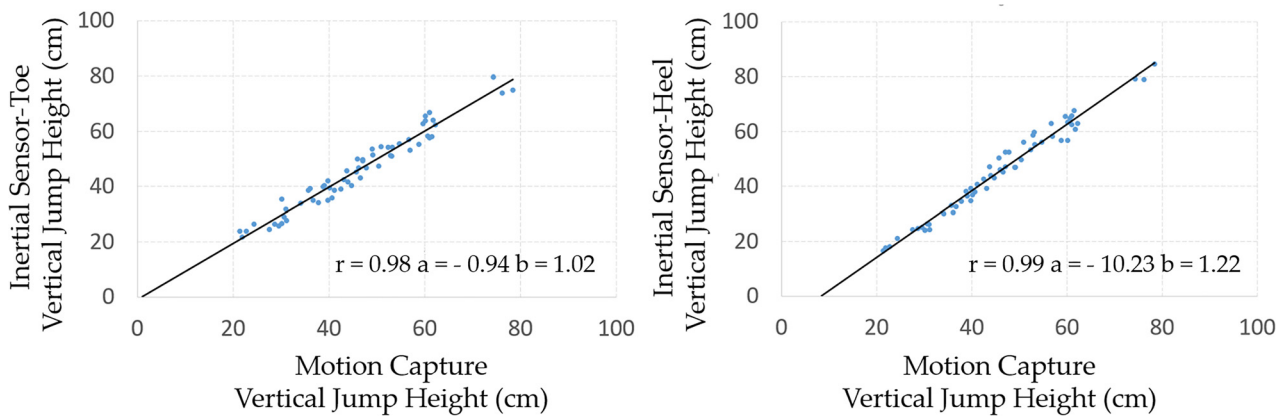

Fig. 4 Linear regression of jump height estimation between inertial and optical motion capture sensing at the (left) toe and (right) heel. *r* is the correlation coefficient, *a* is the regression intercept, and *b* is the regression slope.

(a) does not include 0. And Pearson's correlation coefficient (r) was used to characterize the association of the regression.

4 Results

Average vertical jump height errors from inertial sensor at the toe and heel were -2.2 ± 2.1 cm and -0.4 ± 3.8 cm (Fig. 4). Absolute agreements, as measured using ICCs between the motion capture system and inertial sensor at the toe (ICC(2,1) = 0.98) and heel (ICC(2,1) = 0.97) were classified as "excellent" as defined by Bland and Altman [48]. The linear regressions were highly correlated between the motion capture system and the inertial sensor at the toe ($r = 0.98$) and heel ($r = 0.99$) (Fig. 4). No proportional bias ($b = 1.02$) or fixed bias ($a = -0.94$) were detected in vertical jump height estimations for the inertial sensor at the toe, but proportional bias ($b = 1.22$) and fixed bias ($a = -10.23$) were detected for the inertial sensor at the heel. Typical vertical acceleration profiles at the toe and heel are shown in Figs. 4(*a*) and 4(*b*), respectively (see Supplemental Material which is available under the "Supplemental Data" tab for this paper on the Digital Collection).

5 Discussion

The purpose of this study was to present and validate a vertical jump height estimation algorithm based on vertical acceleration profiles during a countermovement jump from foot-worn inertial sensing. Results demonstrated that the algorithm has excellent agreement with the gold standard optical motion capture system measurements.

These findings contribute to the existing body of research aimed at estimating vertical jump height. This algorithm was more accurate than nonoptical landmark based methods, such as from Vertec [15] and other IMU-based devices like Myotest [31] and achieved similar accuracy as contact mat-based systems like Just Jump [15]. Dowling et al. [27] used flight time equations based on shank-mounted accelerometer and reported high precision but the sensor needs to be attached to skin, which could be inconvenient and cause discomfort. Picerno et al. [25] developed an algorithm based on a trunk-mounted accelerometer that was relatively accurate; however, the algorithm was more sensitive to sensor alignment and the accuracy of accelerometer data since the height and velocity was determined by double numerical integration of the vertical acceleration component [49,50]. In addition, previous IMU-based approaches [29,32] typically only used the local vertical axis of the inertial sensor instead of the global vertical acceleration to determine flight time, which could cause significant estimation errors if the local sensor vertical axis is not perfectly aligned with the global gravity axis. Because this algorithm is based on vertical acceleration signal, it is insensitive to orientation misalignment. This provides practical advantages for implementation outside of a laboratory setting. Compared with existing torso-based methods, foot mounted-accelerometers could also be used in other applications, such as for gait phase detection [34] and for estimating walking energy [35] or running speed [36].

While no bias was detected in the estimations via inertial sensor at the toe, there was proportional bias and fixed bias for estimations at heel. This may be because of the algorithm assumption that takeoff time is approximately the midpoint of the falling edge of the acceleration impulse, which seems to hold for inertial sensors at the toe but not the heel. Given that the heel and toe present different accuracy and variability performance characteristics, combining both sensors could enhance their collective predictive accuracy. Future research should be conducted to develop an algorithm utilizing both toe and heel sensors simultaneously to potentially further improve jump height accuracy.

While actual and theoretical acceleration profiles followed the same general form, there were some notable differences (Figs. 5(*a*) and 5(*b*)). During the take-off phase, there was typically a small impulse before takeoff, caused by small motion of the toe during the preliminary downward movement. Also, after takeoff, the acceleration did not decrease directly to $-g$. The waves were likely caused by the resonance of the elastic materials inside the inertial sensor. Finally, during the landing phase, the acceleration profile displayed several impulses rather than one, which is likely because either subjects cannot stand firmly as soon as landing or the inertial sensing unit bounces up and down directly after ground contact. As mentioned in Sec. 2.3, these differences did not affect the detection of takeoff/landing characteristics or the accuracy of the algorithm. Given that the amplitude of resonance does not generally exceed the peak or trough during the takeoff/landing impulse, we did not use any signal processing. Nevertheless, signal processing could still be added and used to improve accuracy.

A limitation of this study is that we only tested healthy participants with standard countermovement jump patterns, thus, the accuracy of the algorithm may vary for abnormal jumping such as in patients who have undergone surgery after Achilles tendon rupture, which could affect the algorithm accuracy. Besides, the required accuracy is application specific and can vary. For example, significant strength improvements result in 5–10 cm increases in vertical jump for basketball players [9], and significant injury recovery improvement from soccer is marked by a 2 cm increase in vertical jump [8]. Thus, this algorithm in its current form may not be suitable for all applications. Several approaches could be used in the future to further improve accuracy such as targeted signal processing, increasing sampling frequency, and utilizing both toe and heel sensors simultaneously. The performance should be similar for comparable or higher performing accelerometers; however, it is possible that accuracy could decrease for inferior accelerometers with more noise or lower sampling rates, for

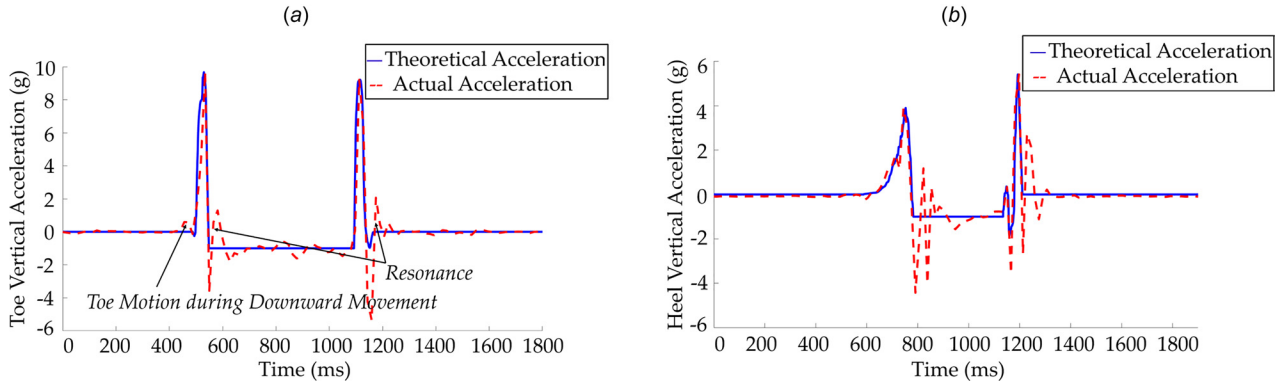

Fig. 5 (*a*) Typical trial for toe theoretical and actual vertical acceleration profiles. (*b*) Typical trial for heel theoretical and actual vertical acceleration profiles.

instance. More studies are needed to validate this algorithm on lower quality accelerometers. Another potential limitation is that this algorithm was validated for isolated, vertical jumps as are often used to benchmark performance or recovery intervention [8,11]. However, more research should be conducted to validate algorithm performance for nonisolated, nonperfectly vertical jumps.

In conclusion, the presented algorithm shows excellent reliability as compared to motion capture and offers the possibility of estimating maximum vertical jump height using foot-worn inertial sensing. Because of its simplicity and low cost, the method could potentially be suitable for sports such as for training in soccer or basketball [7,9] or for clinical evaluation [13,51]. This validated algorithm also enables jump height estimation outside of traditional optical marker-based movement analysis laboratories and clinics.

Acknowledgment

The authors would like to thank Carmichael Ong for his advice in performing vertical jump dynamic simulations via OpenSim.

Funding Data

- This work was supported by the National Natural Science Foundation of China (Grant Nos. 51505283 and 51650110491).

References

[1] Gallahue, D. L., and Ozmun, J. C., 2002, *Understanding Motor Development: Infants, Children, Adolescents, Adults*, McGraw-Hill, New York, pp. 131–139.
[2] Harrison, A. J., and Gaffney, S., 2001, "Motor Development and Gender Effects on Stretch–Shortening Cycle Performance," J. Sci. Med. Sport, **4**(4), pp. 406–415.
[3] Bosco, C., and Komi, P. V., 1980, "Influence of Aging on the Mechanical Behaviour of Leg Extensor Muscles," Eur. J. Appl. Physiol., **45**(2), pp. 209–219.
[4] De Vito, G., Bernardi, M., Forte, R., Pulejo, C., Macaluso, A., and Figura, F., 1998, "Determinants of Maximal Instantaneous Muscle Power in Women Aged 50–75 Years," Eur. J. Appl. Physiol., **78**(1), pp. 59–64.
[5] Foldvari, M., Clark, M., Laviolette, L. C., Bernstein, M. A., Kaliton, D., and Castaneda, C., 2000, "Association of Muscle Power With Functional Status in Community-Dwelling Elderly Women," J. Gerontol.: Ser. A, **55**(4), pp. 192–199.
[6] Kasovic, M., Pribanic, T., and Medved, V., 2002, "Take-Off and Landing Properties in Top-Level Football Players: A Ground Reaction Force Study. Kinesiology," Int. J. Fundam. Appl. Kinesiology, **34**(2), pp. 182–191.
[7] Wisloff, U., Castagna, C., Helgerud, J., Jones, R., and Hoff, J., 2004, "Strong Correlation of Maximal Squat Strength With Sprint Performance and Vertical Jump Height in Elite Soccer Players," Br. J. Sports Med., **38**(3), pp. 285–288.
[8] Tessitore, A., Meeusen, R., Cortis, C., and Capranica, L., 2007, "Effects of Different Recovery Interventions on Anaerobic Performances Following Preseason Soccer Training," J. Strength Cond. Res., **21**(3), pp. 745–750.
[9] Ziv, G., and Lidor, R., 2010, "Vertical Jump in Female and Male Basketball Players: A Review of Observational and Experimental Studies," J. Sci. Med. Sport, **13**(3), pp. 332–339.
[10] Bobbert, M. F., Gerritsen, K. J., Litjens, M. C., and Van-Soest, A. J., 1996, "Why Is Countermovement Jump Height Greater Than Squat Jump Height?," Med. Sci. Sports Exercise, **28**(11), pp. 1402–1412.
[11] Viitasalo, J. T., Rahkila, P., Oesterback, L., and Alen, M., 1992, "Vertical Jumping Height and Horizontal Overhead Throwing Velocity in Young Male Athletes," J. Sports Sci., **10**(5), pp. 401–413.
[12] Myer, G. D., Ford, K. R., Palumbo, J. P., and Hewett, T. E., 2005, "Neuromuscular Training Improves Performance and Lower-Extremity Biomechanics in Female Athletes," J. Strength Cond. Res., **19**(1), pp. 51–60.
[13] Petschnig, R., Baron, R., and Albrecht, M., 1998, "The Relationship Between Isokinetic Quadriceps Strength Test and Hop Tests for Distance and One-Legged Vertical Jump Test Following Anterior Cruciate Ligament Reconstruction," J. Orthop. Sports Phys. Ther., **28**(1), pp. 23–31.
[14] Sargent, D. A., 1921, "The Physical Test of a Man," Am. Phys. Educ. Rev., **26**(4), pp. 188–194.
[15] Leard, J. S., Cirillo, M. A., Katsnelson, E., Kimiatek, D. A., Miller, T. W., and Trebincevic, K., 2007, "Validity of Two Alternative Systems for Measuring Vertical Jump Height," J. Strength Cond. Res., **21**(4), pp. 1296–1299.
[16] Dal Monte, A., and Mirri, G., 1996, "The Functional Evaluation of the Athlete: Methods and State of the Art," Med. Sport (Turin), **49**(3), pp. 323–336.
[17] Sébert, P., Barthélémy, L., Dietman, Y., Douguet, C., and Boulay, J., 1990, "A Simple Device for Measuring a Vertical Jump: Description and Results," Eur. J. Appl. Physiol. Occup. Physiol., **61**(3–4), pp. 271–273.
[18] Aragón-Vargas, L. F., 1997, "Kinesiological Factors in Vertical Jump Performance: Differences Among Individuals," J. Appl. Biomech., **13**(1), pp. 24–44.
[19] Bobbert, M. F., Huijing, P. A., and Van Ingen Schenau, G. J., 1987, "Drop Jumping. I. The Influence of Jumping Technique on the Biomechanics of Jumping," Med. Sci. Sports Exercise, **19**(4), pp. 332–338.
[20] Pandy, M. G., and Zajac, F. E., 1991, "Optimal Muscular Coordination Strategies for Jumping," J. Biomech., **24**(1), pp. 1–10.
[21] Bobbert, M. F., and Van Soest, A. J., 1994, "Effects of Muscle Strengthening on Vertical Jump Height: A Simulation Study," Med. Sci. Sports Exercise, **26**(8), pp. 1012–1020.
[22] Asmussen, E., and Bonde-Petersen, F., 1974, "Storage of Elastic Energy in Skeletal Muscles in Man," Acta Physiol., **91**(3), pp. 385–392.
[23] Bosco, C., Luhtanen, P., and Komi, P. V., 1983, "A Simple Method for Measurement of Mechanical Power in Jumping," Eur. J. Appl. Physiol., **50**(2), pp. 273–282.
[24] Dowling, J. J., and Vamos, L. J., 1993, "Identification of Kinetic and Temporal Factors Related to Vertical Jump Performance," J. Appl. Biomech., **9**(2), pp. 95–110.
[25] Picerno, P., Camomilla, V., and Capranica, L., 2011, "Countermovement Jump Performance Assessment Using a Wearable 3D Inertial Measurement Unit," J. Sports Sci., **29**(2), pp. 139–146.
[26] Menzel, H. J., Chagas, M. H., Szmuchrowski, L. A., Araujo, S. R., Campos, C. E., and Giannetti, M. R., 2010, "Usefulness of the Jump-and-Reach Test in Assessment of Vertical Jump Performance," Perceptual Mot. Skills, **110**(1), pp. 150–158.
[27] Dowling, A. V., Favre, J., and Andriacchi, T. P., 2011, "A Wearable System to Assess Risk for Anterior Cruciate Ligament Injury During Jump Landing: Measurements of Temporal Events, Jump Height, and Sagittal Plane Kinematics," ASME J. Biomech. Eng., **133**(7), p. 071008.
[28] Chardonnens, J., Favre, J., Le Callennec, B., Cuendet, F., Gremion, G., and Aminian, K., 2012, "Automatic Measurement of Key Ski Jumping Phases and Temporal Events With a Wearable System," J. Sports Sci., **30**(1), pp. 53–61.
[29] Quagliarella, L., Sasanelli, N., Belgiovine, G., and Cutrone, N., 2006, "Flying Time Evaluation in Standing Vertical Jump by Measurement of Ankle Accelerations," Gait Posture, **24**(24), pp. 56–57.

[30] Palma, S., Silva, H., Gamboa, H., and Mil-Homens, P., 2008, "Standing Jump Loft Time Measurement: An Acceleration Based Method," Biosignals, **2**, pp. 393–396.
[31] Casartelli, N., Müller, R., and Maffiuletti, N. A., 2010, "Validity and Reliability of the Myotest Accelerometric System for the Assessment of Vertical Jump Height," J. Strength Cond. Res., **24**(11), pp. 3186–3193.
[32] Innocenti, B., Facchinelli, D., Torti, S., and Verza, A., 2006, "Analysis of Biomechanical Quantities During a Squat Jump: Evaluation of a Performance Index," J. Strength Cond. Res., **20**(3), pp. 709–715.
[33] Le, N. N. N., and Cavallaro, A., 2015, "Basketball Activity Recognition Using Wearable Inertial Measurement Units," XVI International Conference on Human Computer Interaction, Vilanova i la Geltrú, Spain, Sept. 7–9, p. 60.
[34] Pappas, I. P. I., Keller, T., Mangold, S., Popovic, M. R., Dietz, V., and Morari, M. A., 2004, "Reliable Gyroscope-Based Gait-Phase Detection Sensor Embedded in a Shoe Insole," IEEE Sens. J., **4**(2), pp. 268–274.
[35] Orecchini, G., Yang, L., Tentzeris, M. M., and Roselli, L., 2011, "Smart Shoe: An Autonomous Inkjet-Printed RFID System Scavenging Walking Energy," IEEE International Symposium on Antennas and Propagation (APS), Spokane, WA, July 3–8, pp. 1417–1420.
[36] McClusky, M., 2009, "The Nike Experiment: How the Shoe Giant Unleashed the Power of Personal Metrics," Wired Mag., **17**(1), pp. 81–91.
[37] Bae, J., and Tomizuka, M., 2013, "A Tele-Monitoring System for Gait Rehabilitation With an Inertial Measurement Unit and a Shoe-Type Ground Reaction Force Sensor," Mechatronics, **23**(6), pp. 646–651.
[38] Sadi, F., Klukas, R., and Hoskinson, R., 2013, "Precise Air Time Determination of Athletic Jumps With Low-Cost MEMS Inertial Sensors Using Multiple Attribute Decision Making," Sports Technol., **6**(2), pp. 63–77.
[39] Patel, S., Park, H., Bonato, P., Chan, L., and Rodgers, M., 2012, "A Review of Wearable Sensors and Systems With Application in Rehabilitation," J. Neuroeng. Rehabil., **9**(12), pp. 1–17.
[40] Tunca, C., Pehlivan, N., Ak, N., Arnrich, B., Salur, G., and Ersoy, C., 2017, "Inertial Sensor-Based Robust Gait Analysis in Non-Hospital Settings for Neurological Disorders," Sensors, **17**(4), p. 825.
[41] Aragón, L. F., 2000, "Evaluation of Four Vertical Jump Tests: Methodology, Reliability, Validity, and Accuracy," Meas. Phys. Educ. Exercise Sci., **4**(4), pp. 215–228.
[42] Delp, S. L., Anderson, F. C., Arnold, A. S., Loan, P., Habib, A., John, C. T., Guendelman, E., and Thelen, D. G., 2007, "OpenSim: Open-Source Software to Create and Analyze Dynamic Simulations of Movement," IEEE Trans. Biomed. Eng., **54**(11), pp. 1940–1950.
[43] Nicholson, K., Jagadish, A. K., and Sensortec, B., 2014, "Sensor Fusion Enhances Device Performance," *Sensor Fusion Bosch Performance Sensortec Accuracy*, Bosch Sensortec, Baden-Württemberg, Germany.
[44] Sensortec, B., 2016, "BNO055 Intelligent 9-Axis Absolute Orientation Sensor," Bosch Sensortec, Baden-Württemberg, Germany.
[45] Sensortec, B., 2014, "BMX055 Small, Versatile 9-Axis Sensor Module," Bosch Sensortec, Baden-Württemberg, Germany.
[46] Clark, R. A., Bryant, A. L., Pua, Y., McCrory, P., Bennell, K., and Hunt, M., 2010, "Validity and Reliability of the Nintendo Wii Balance Board for Assessment of Standing Balance," Gait Posture, **31**(3), pp. 307–310.
[47] Ludbrook, J., 2002, "Statistical Techniques for Comparing Measurers and Methods of Measurement: A Critical Review," Clin. Exp. Pharmacol. Physiol., **29**(7), pp. 527–536.
[48] Bland, J. M., and Altman, D. G., 1990, "A Note on the Use of the Intraclass Correlation Coefficient in the Evaluation of Agreement Between Two Methods of Measurement," Comput. Biol. Med., **20**(5), pp. 337–340.
[49] Thong, Y. K., Woolfson, M. S., Crowe, J. A., Hayes-Gill, B. R., and Jones, D. A., 2004, "Numerical Double Integration of Acceleration Measurements in Noise," Measurement, **36**(1), pp. 73–92.
[50] Koster, T., and Lambeck, P., 2002, "Dependence of Inertial Measurements of Distance on Accelerometer Noise," Meas. Sci. Technol., **13**(8), pp. 1163–1172.
[51] Laudner, K., Evans, D., Wong, R., Allen, A., Kirsch, T., Long, B., and Meister, K., 2015, "Relationship Between Isokinetic Knee Strength and Jump Characteristics Following Anterior Cruciate Ligament Reconstruction," Int. J. Sports Phys. Ther., **10**(3), pp. 272–280.